

Aerodynamics and Radar Signature: A Combination of Theoretical Methods

Stephen M. Hitzel*

Dornier GmbH, Friedrichshafen, Federal Republic of Germany

Combat aircraft are threatened by radar-controlled anti-aircraft systems. Knowledge of the scattering of electromagnetic waves from aircraft allows aerodynamic designers to design a low radar signature or to improve the tactics of aircraft in service to successfully avoid enemy defensive reaction. A theoretical approach is presented to estimate the radar signatures of complex aircraft configurations including external stores. The signature is evaluated by determining the radar cross sections of intended radar-observation directions. The radar cross section of a certain aspect view of a radar observation is evaluated by combining specular geometrical and physical optics for curved-surface elements, such as wing surfaces, that are large with respect to the radar's wavelength. Diffraction formulas are added to introduce the radar-reflection characteristics of edges. The geometric input is equal to the buildup of usual aerodynamic panel methods and, by the evaluation of the panels' principal curvatures by higher-order means, allows the regard of the curved aircraft surfaces. The diffractions typical for edges (wing edges, etc.) are included with regard to the edges' sharpness and geometric shape. The total radar cross section is determined by summing up all reflecting areas (by the combination of the contributing panels) and edge elements. Thus, an aerodynamic surface discretization can be used without modification. The signatures of principal bodies and a fighter aircraft, both armed and unarmed, when exposed to a typical radar illumination, are presented.

Nomenclature

A	= antenna area
a	= typical dimension
e	= antenna efficiency
\vec{E}	= electromagnetic field vector
G	= antenna gain
L	= edge length
P	= power transmitted
R	= range
r	= edge radius (e.g., wing leading-edge radius)
S	= signal strength
λ	= wavelength
α	= local azimuth of an edge
ϕ	= elevation
θ	= azimuth

Subscripts

SC	= local scatterer
S	= due to scattered field
I	= due to incident field

I. Introduction

THE demands on survivability of combat aircraft and the pursuit of their missions emphasize the necessity to reduce their radar signature.¹ The radar signature is the portion of electromagnetic signals scattered into the direction of a radar receiver. The size of the signature is referred to as the radar cross section (RCS)²⁻⁵ and is derived as depicted in Fig. 1.

RCS describes the fraction of the electromagnetic radiation scattered to the receiver with respect to the impinging radar signal. It depends strongly upon the aspect view of the illumi-

nating and observing radar system with respect to the aircraft. In case of monostatic systems, when the directions of illumination and observation are identical, the RCS is referred to as backscatter RCS. The RCS of bistatic systems, which means that the radar transmitter and receiver are not collocated, is not discussed here. RCS also depends on the wavelength and the polarization of the threat radar. Since the aircraft's shape and its structure form a reflector for the illuminating radar rays, RCS is significantly affected by the aircraft's configuration, its structure, and its materials.

Ever increasing radar threats demand improvements in active counter measures (jamming) that finally may increase the consumption of electric power.¹ These installations will affect the aircraft's weight and drag at the expense of its overall performance.

Apart from those active radar countermeasures, the aircraft designer can only affect backscattered signals on the aircraft itself. This can be done by means of the electromagnetic properties of the materials used and/or by the shape and size of the aircraft configuration. For typical air defense radars operating with wavelengths that are small compared with their target's individual reflecting surfaces in the so-called optical region, shaping can be very effective for reducing RCS.

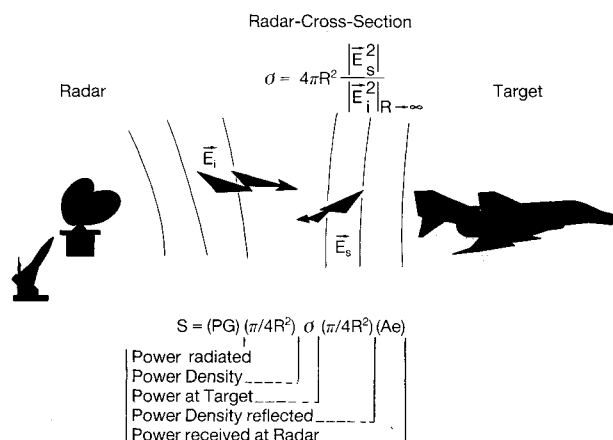


Fig. 1 Influence of RCS σ on the radar signal.

Presented as Paper 86-1770 at the AIAA 4th Applied Aerodynamics Conference, San Diego, CA, June 9-11, 1986; received July 30, 1986; revision received June 1, 1987. Copyright © American Institute of Aeronautics and Astronautics, Inc., 1986. All rights reserved.

*Dipl.-Ing., Research Scientist in Theoretical Aerodynamics. Member AIAA.

Horten Ho IX 1944

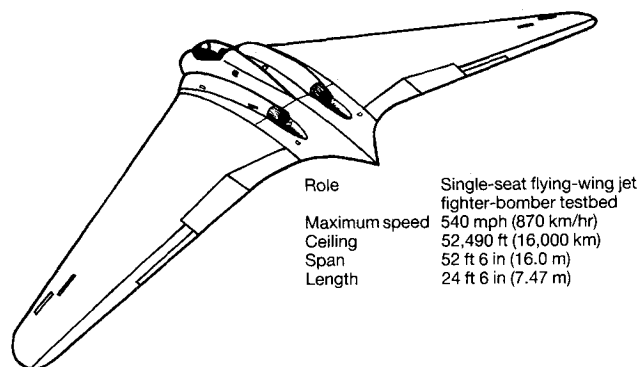


Fig. 2 Combining aerodynamic efficiency and radar cross-section reduction.

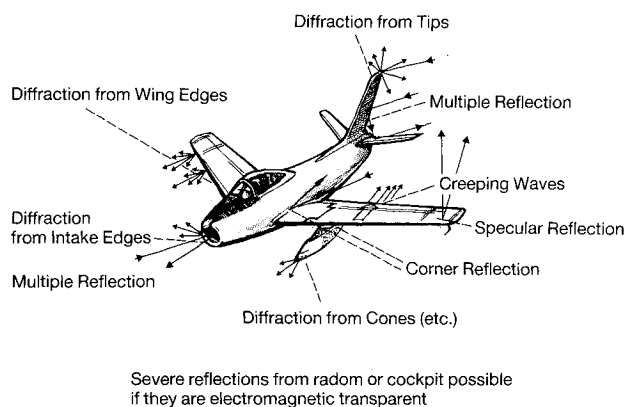


Fig. 3 Some electromagnetic scattering mechanisms typical for an aircraft configuration.

Thus, the aerodynamic designer is concerned with the problem of combining both an efficient aerodynamic shape and the shape of an inefficient radar reflector⁶ with respect to anticipated radar illumination. Figure 2 depicts one of the very first more or less accidental attempts—in 1944 by the flying jet wing Horten Ho IX⁷ in Germany—to combine a very efficient aerodynamic shape with a low radar-signature configuration.

As stated in Fig. 1, the detection range of a radar system depends on the power radiated within a certain beam, the effective size of its radar antenna, and the target's RCS. Knowledge of the nature of the radar signature and its specific sources—the local contributions of RCS—on the aircraft itself allows aerodynamic designers to design aircraft or to conceive tactics that can avoid defense system's reaction in time. Figure 3 depicts some of the most common electromagnetic scattering mechanisms on a typical aircraft configuration.

Many of the mechanisms mentioned in Fig. 3 can be reduced or even avoided by some basic ideas on shaping. Thus, strong multireflections from rectangular corners and diffractions from edges whose characteristic geometric shapes may cause resonance for the impinging radar waves must be avoided. The use of blended wing-fuselage configurations may get rid of severe reflections springing from rectangular corners. Sharp and/or nonstraight edges (wings, intake lips, nozzles, splitter plates, etc.) suppress intense antenna-type diffractions. Long curved intake ducts help to avoid direct backscattering from the engine's first compressor stage. Blended cockpits and radoms prevent strong multireflections from interior boxes and structures. Also, large surfaces directed normally to the front- and sideview (e.g., vertical tails) should be avoided. Naturally, the same is true for external pylon-mounted stores. Pylons and stores significantly contribute to the signature by specular and corner reflections

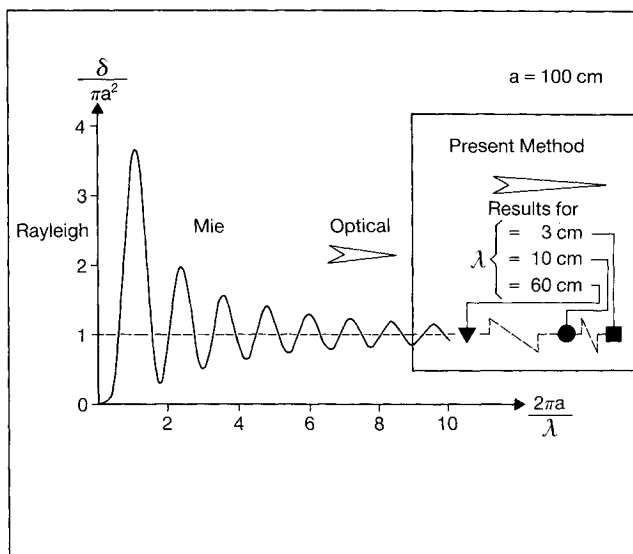


Fig. 4 RCS of a conducting sphere⁹ as a function of the wavelength.

and edge diffractions. Conformal stores could camouflage some intense areas of reflection, while internal carriage should do away with the store's radar problem. References 6 and 8 give more details.

Some of the means of radar-signature shaping go hand in hand with efficient aerodynamic shapes, especially for high-speed design.⁶ For instance, blended wing-fuselage shapes allow proper volume distributions for supersonic flight. So do internal stores. Supersonic intake cones prevent the direct illumination of compressors and provide good precompression at reduced intake losses. Thus, well-balanced designs combining both efficient aerodynamics and favorable radar shaping may provide configurations with enhanced survivability.

II. Theoretical Approaches to Radar Signature

The prediction and measurement of RCS, with respect to the complete determination of an aircraft's radar signature, is a very difficult task. RCS measurements demand enormously large radar ranges with respect to the aircraft's size to simulate full-scale relations as closely as possible. An experimental alternative is an apparatus providing the proper model relations, materials, and structures with regard to the relation of the simulated wavelengths and the model's scale. Depending only on the experimental approach may be very laborious and costly for design purposes.

Theory provides another tool to evaluate RCS. By solving the complete Maxwell equations bound into appropriate boundary conditions for a given target's geometry, the complex electromagnetic field can be determined.^{2,4} RCS, the relation of the impinging and reflected electric or magnetic field vectors, can be evaluated according to Fig. 1. The result will include all electromagnetic properties within the Rayleigh, Mie, and optical regions.

In the Rayleigh region where the wavelength λ is larger than a typical length a , the target's RCS increases with decreasing λ . In the Mie region where $\lambda \approx a$, RCS is heavily dependent on λ . In the optical region where λ is less than a , RCS is basically independent of λ . The relation of RCS with respect to a/λ is depicted in Fig. 4 for the example of a sphere.⁹

Figure 5 helps to give a survey of methods to evaluate the electromagnetic properties of bodies and/or the corresponding RCS. The most physical approach, naturally, is the field solution of the complete Maxwell equations, which would include all electromagnetic effects including dielectric and other inhomogeneous properties. The geometric grid necessary for the evaluation of bodies exposed to electromagnetic radiation must be very fine. At least several grid points are necessary to allow the proper resolution of the illumination's wavelength.



Mathematical Models for RCS Determination		
Method	Equations	Application
Field Methods	Maxwell	
Surface-Methods "Classical"	Vector-Helmholtz (Integraleq.)	Simple Bodies
GTD Geomet. Theo. of Diffraction	Simplified Integraleq. Surface Int. and Optical EQ	Large Wavelength
PO Physical Optics GO Geometr. Optics		Short Wavelength
Superposition of Solutions of Basic Bodies and Effects		Few Multireflections
	Superpos. Formula	
		Large Configurations Engineering Methods

Fig. 5 Theoretical approaches for the evaluation of RCS.

This can involve large computer time and storage. Since the solution of the complete Maxwell equations still is rather costly on today's computers, even for simple configurations with the assumption of perfectly conducting surfaces, numerous simplifications have been developed. Reference 10 gives a good account of these.

The reduction of the Maxwell equations (see Refs. 2, 3 and 11) to the solution of the vector-Helmholtz equations (Fig. 5) by panel methods and/or source-distribution methods, which usually are limited to large wavelengths rather than short ones, demand very large matrices to be solved in a numerical solution procedure. In the near future, simplified approaches using field methods that result in lower computer time and storage may become competitive right here. Additional simplifications for the theory of geometrical diffraction down to physical and geometrical optics provide effective tools for RCS prediction but at the expense of neglected electromagnetic effects. Thus, source-distribution methods neglect tip and edge diffraction and creeping waves. They are economical only for large wavelengths. Physical optics loose on polarization, while ray tracing is difficult for multireflections in a geometrical optics approach.

The superposition of solutions³⁻⁵ for basic shapes overcomes some difficulties of the aforementioned tools by the piecewise approximation of the target geometry with basic bodies. This method allows only a first guess of RCS; however, it provides effective engineering methods for complex geometries.

The aerodynamic designer, interested in a first guess of RCS, needs a theoretical method to get an idea of the radar reflections of the aerodynamic shapes. For ease of use and good correlation of aerodynamic and RCS estimations, both should be done with the same geometric definition. Since most military radars operate in the optical region where the wavelength usually is smaller than typical target dimensions, a theoretical approach for RCS estimation should be valid primarily in the optical region.

III. Basic Concept of the Method Presented

The method presented here starts from the very bottom line of the aforementioned theoretical methods. Figure 5 also gives a crude idea of the capabilities of the mentioned methods compared with the complexity of geometric shapes. For design purposes of complex aircraft geometries, the upper methods in Fig. 5 are still far from being cost-effective for complete radar signatures. Although the middle ones give away many physical effects despite intense calculations, the decomposition of aircraft into simple bodies ends up with an estimation of geometries that are not always compatible with the aerodynamic shapes.

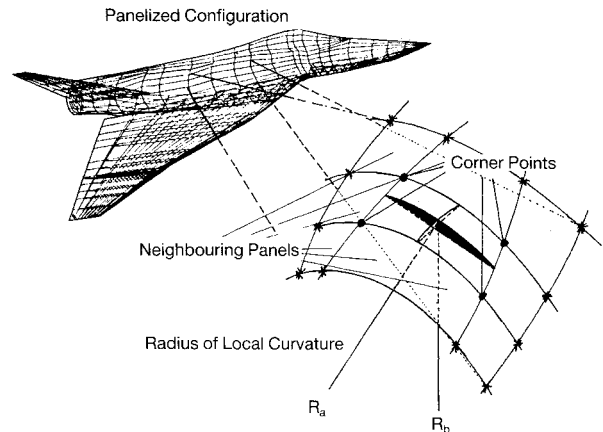


Fig. 6 Least-square-fit to determine surface curvatures.

The approach presented here starts from a geometric basis similar to the input of aerodynamic panel methods to evaluate aerodynamic derivatives or flowfield effects. This allows the use of the identical geometric data for both aerodynamic and RCS evaluations, possibly for combined design procedures. The geometry may include external stores and pylons. Stores of any kind (missiles, bombs, etc.) can be added easily and are treated in the same way as the aircraft's configuration elements are. The signature is evaluated by the calculation of the RCSs of intended aspect views in any elevation and azimuthal direction.

The procedure considers the surface curvature of all aircraft components. While the complete configuration is built up by panel-type surfaces, the panel's curvatures are evaluated by a least-square-fit method resulting in the principal curvatures (R_A and R_B). By taking into account neighboring surface points (Fig. 6) of adjacent panels, a second-order curvature is determined.^{1,3} The varying sharpness of wing edges, for example, can be specified either within the input or from a two-dimensional determination from points near the edges. In the present state, the surfaces of any configuration are assumed to be perfectly conductive.

The radar cross section is determined by combining specular, geometrical, and physical optics. This holds well for the assumption that target dimensions are large with respect to the radar's wavelength. As already stated, this is a reasonable approximation since most military radars operate in the optical region.

The additional evaluation of the electromagnetic characteristics of configuration elements that are small compared to the illumination wavelength (e.g., edges or tips, etc.) allows the inclusion of the most important diffraction effects. Even the influences of wing edges, intake lips and nose tips, etc., can be included. In the procedure, their contributions are included as local scatterers.

A brief description of the means to evaluate scatterers such as wing surfaces, etc., that are large compared to the wavelengths follows now. Afterwards, the means to determine the contributions of elements such as edges, etc., are outlined.

Assuming infinite distance off a radar source results in impinging electromagnetic wave fronts being plane. Since the procedure is provided only for very high frequencies with respect to short wavelengths, the influence of adjacent, radar-induced, interfering surface currents can be neglected. According to physical optics, the influence of the induced surface currents causing reflection is restricted locally. In shadowed regions, the surface currents are assumed to be zero. Only visible surfaces contribute to RCS. Thus, a "hidden surface" procedure is used to determine the areas capable of reflecting rays in the direction of observation. The reflection of radar rays is determined by the simple means of geometrical optics for pure reflection.

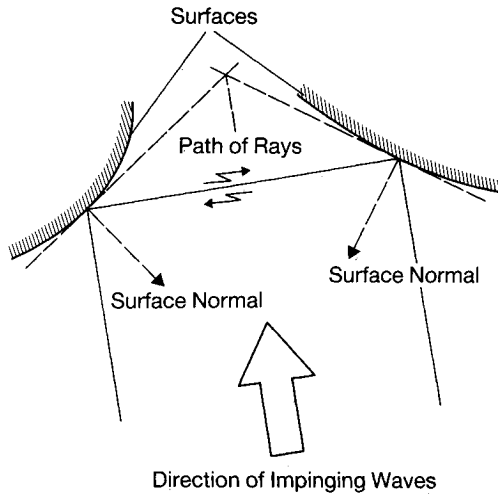


Fig. 7 Simple double reflection.

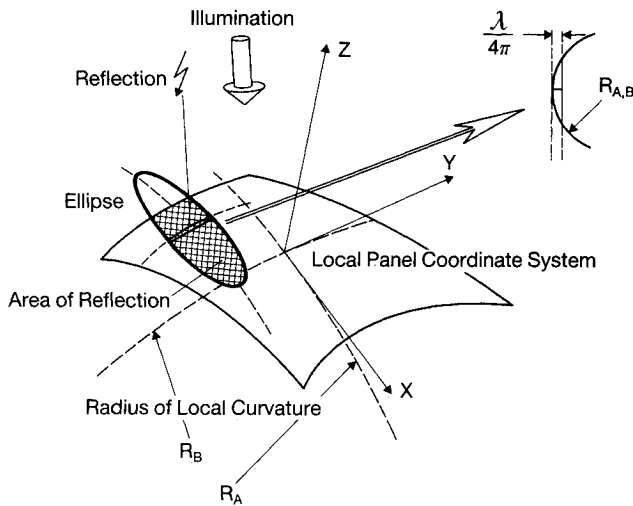


Fig. 8 Area of reflection on a second-order curved surface.

Multireflections between several components are not considered, since ray tracing may become very laborious and expensive. However, a simple double-reflection procedure is outlined in Fig. 7. Scanning for surfaces whose combined normal directions form a vector into the radar-observation direction provides a simple means for including double reflections.

References 3 and 4 describe in more detail the simplifications and assumptions necessary to find the way down to physical and geometrical optics.

The evaluation of surface reflections is determined by a method similar to that stated by Ref. 5. The following will be repeated for all visible panels. The center of the reflection with respect to a panel is found by evaluating the position of the surface-normal vector that is parallel to the direction of the radar observation. This position must not be within the panel being used in the procedure, since the panel itself is only a part of the surface of interest. One fourth of the illuminating wavelength cuts out caps from the curved surfaces, of which the treated panel may be only a part, as described by Fig. 8.

Since the local surface curvature, which is identical to the panel's principal curvature, is determined by two orthogonal radii, the base of every cap is of elliptical shape. The portion that overlaps the area of the treated panel is identical to the surface contributing to RCS. For flat surfaces, the radii of the curvatures become infinite, extending the ellipse to infinity. In this case, the overlapping area would become equal to the panel's surface. Adding up all the panels' reflecting areas results in the contribution of the aircraft's surface elements to RCS.

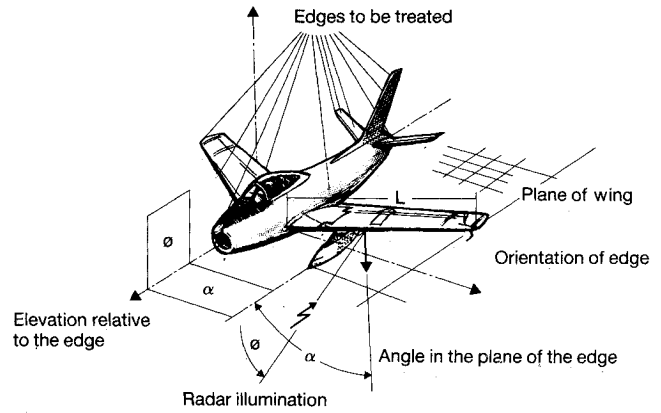


Fig. 9 Diffraction from edges, formula from Ref. 4.

Since aircraft configurations include elements whose dimensions are small compared to the illumination's wavelength (e.g., wing edges, nose cones, and/or nose tips), formulations considering the influence of shape and wavelength have to be applied for those. Reference 4 gives some practical formulations for the treatment of different kinds of edges (Fig. 9). For instance, the local RCS of wing, tail, intake, splitter plate, and nozzle edges is determined by the following formula:

$$\sigma_{\text{Edges}} = \frac{\pi L^2 \sin^2 \alpha \left[\frac{\sin M \cos \alpha}{M \cos \alpha} \right]^2 \cos^4 \phi}{\frac{\pi^2}{4} + \left[\ln \left(\frac{\lambda}{N \sin \alpha} \right) \right]^2} \quad (1)$$

where $M = 2\pi L / \lambda$ and $N = 1.78\pi \times r$.

The procedure takes into account varying shapes of any edges. For instance, the influence of curved wing edges or the influence of different intake shapes can be considered.

Other shapes like cones, ogives, or corner reflectors (e.g., wing-body junctions) can be included,³⁻⁵ similar to the procedure described.

The total RCS is obtained by superimposing the local scatterers. This can be done either by a formulation estimating the upper bound when the returns from the target are all in phase.

$$\delta = \left(\sum_{SC=1}^{SC} \sqrt{\delta_{SC}} \right)^2 \quad (2)$$

or by the inclusion of the phase shift¹

$$\delta = \left| \sum_{SC=1}^{SC} \sqrt{\delta_{SC}} \exp(i4\pi R_{SC}/\lambda) \right|^2 \quad (3)$$

Effects of polarization are not taken into account for surfaces that are larger than the illumination's wavelength. Edges, etc., show different patterns of reflection according to polarization. Thus, different formulas for both vertical and horizontal polarization can be used. The given plane of polarization of the electric field vector parallel to an edge causes larger scattering than vertical polarization. To estimate an upper bound for engineering purposes, the parallel polarization is assumed.

IV. Results for Simple and Complex Shapes

Figures 4 and 10 provide a comparison of the method presented with exact theory and experiment. Figure 4, which was already used to describe the typical electromagnetic regions with regard to the relation of the wavelength versus the body's size, also shows some results evaluated by the method for a perfectly conducting sphere. Within the optical region, the results turn out to be exact since the wavelengths are short with respect to the body's size. At longer wavelengths, the procedure no longer holds since the strong relationship between

body size and wavelength is not considered. Figure 10 depicts the experimental results found in Ref. 12. The method described here delivered good results for the frontal and the broadside illumination. However, not all the different peaks in the experimental results are simulated, since no creeping- or traveling-wave effects along the cylinder and no diffraction from discontinuities are considered.

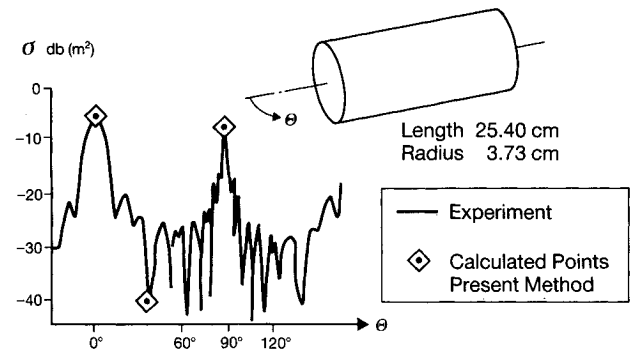


Fig. 10 Signature of a cylinder exposed to 3.059 cm waves, experiment.^{1,2}

Figures 11 and 12 show an unarmed and armed fighter-aircraft configuration investigated by the method. Both weapons of the armed version, on wing-tip and under-wing pylons, are typical short- and medium-range missiles. All surfaces are assumed to be perfectly conductive, including the canopy and the radom. The engine's compressor is assumed not to be in line with the intake duct.

Both configurations are illuminated by a wavelength of 3 cm. Figure 13 shows the radar signatures that include both surface reflections and edge diffractions at an elevation of 0 deg. The azimuth angle ranges from the nose-on position to the illumination from astern. Total RCS is combined by the upper-bound formula for engineering purposes, assuming all returns from the target to be in phase. No corners, tips, or double reflections are simulated here. In the region up to 40 deg azimuth, the difference between angles calculated is 1 deg. In the region from 40 to 180 deg, the difference is selected to 4 deg.

To reveal the influence of edges, Fig. 14 provides the contributions of the edges with respect to the total RCS. In the front aspect, the edges of the air intake dominate the radar signature since the radar rays reflected at surface elements are deflected

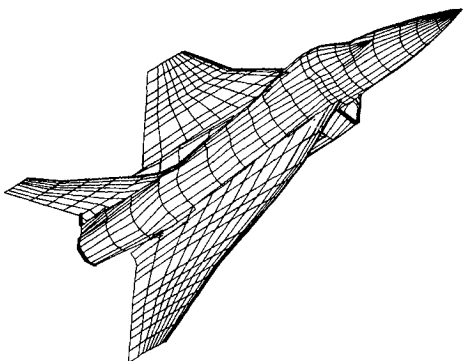


Fig. 11 Unarmed fighter-aircraft configuration.

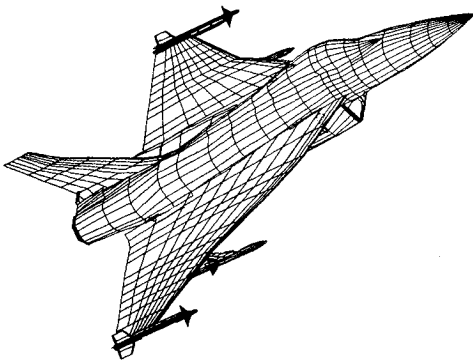


Fig. 12 Armed fighter-aircraft configuration.

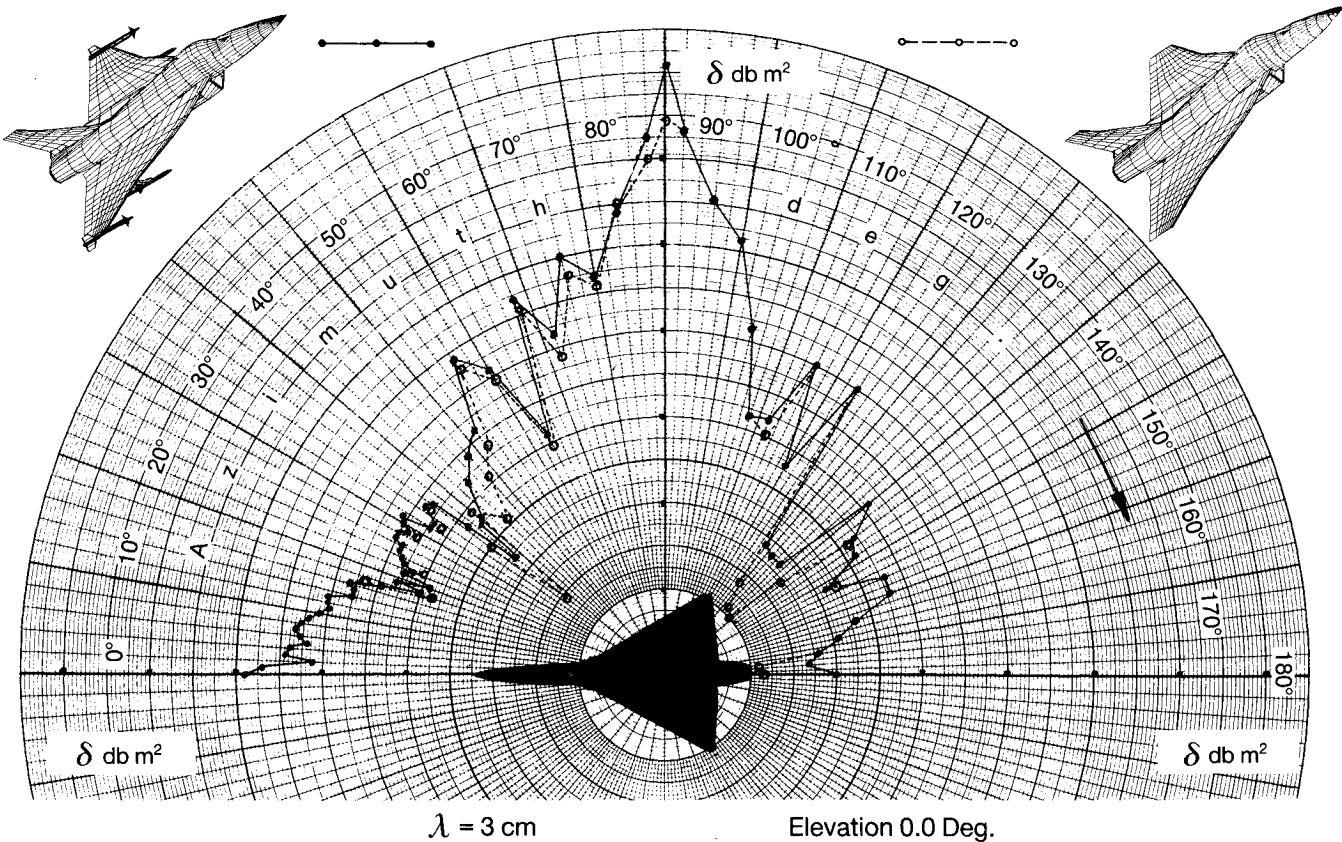


Fig. 13 Radar signatures of an armed and an unarmed fighter aircraft.

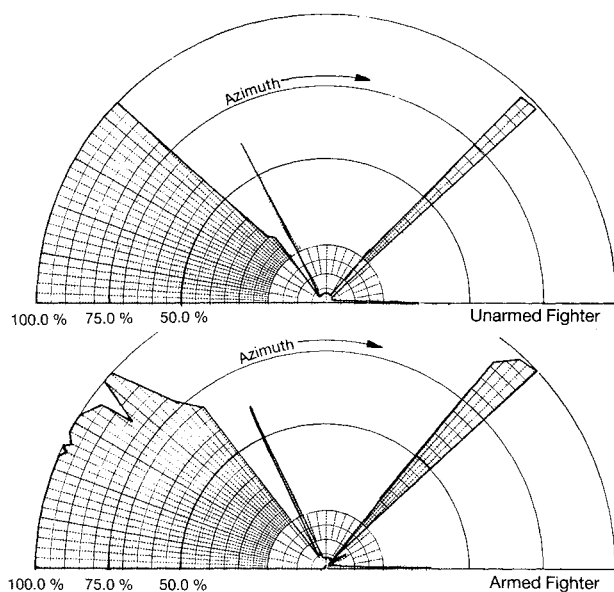


Fig. 14 RCS of edges relative to total RCS.

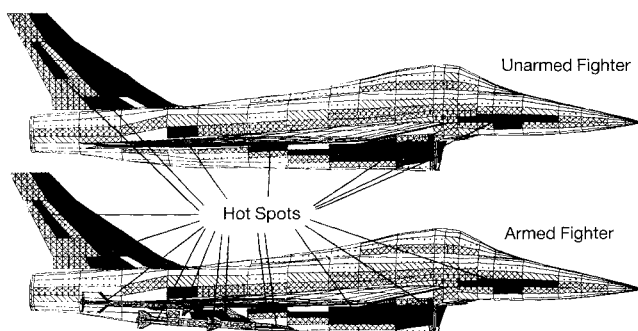


Fig. 15 Radar hot-spots on configurations.

from the line of sight. Since the air intakes of the treated configurations are of the two-dimensional box type, their straight intake lips cause strong diffractions at these edges.

The sharpness of the edges of the intake configuration evaluated accidentally was such that they may be close to the case of a maximum value. For the same wavelength, more sharp or more blunt edges may cause lower contributions. The pronounced peak at approximately 64 deg azimuth corresponds to the sweep of the inner part of the wing's leading edge whose particular sharpness results in lower RCS compared to that of the intake due to a different airfoil sharpness. In the back part at 134 deg, the total RCS is small. This makes the overall contribution of edges large with respect to the total radar signature in this region. The contribution probably is a combination of the trailing-edge root fairing and the jet nozzle, which is also treated by the edge procedure.

The armed configuration reveals additional influence of the pylons and the weapon's trailing edges in this region. The basic configuration dominates the radar signature at the depicted elevation of 0 deg. However, the influence of stores and pylons is also visible. The stores enhance RCS by adding the influence of additional edges and surfaces. The black areas in Fig. 15 mark the local radar hot-spots on both configurations at azimuth 88 deg. Only surface reflections are shown. To simplify presentation, Fig. 15 does not show the exact RCS contribution of each panel surface. Any panel for which a reflection is determined is marked black regardless of the relative size of the real area contributing. The gray areas are potential spots for small changes off the shown aspect view. The additional RCS for the armed configuration is due to the missile's fuselages and the under-wing pylons.

The influence of corners and multireflections is not included here. Those can also have considerable influence on RCS. Provision is made to add other electromagnetic effects typical for corners, some kinds of cones, etc. Any comparison with experimental results is not provided since real aircraft measurements are not available in the open literature.

V. Conclusions

The aerodynamic designer of combat aircraft may have to pay attention to the radar signature of his design in order to enhance its survivability in action. Typical air-defense radars, operating with high frequencies with wavelengths in the optical region, can be degraded in their performance by shaping the aircraft in order to lower its radar signature.

Thus, the aerodynamic designer is concerned with the combination of an efficient aerodynamic shape and an inefficient radar reflector with respect to anticipated radar illumination.

A theoretical approach to determine the RCS that fits well into a typical geometric input of aerodynamic panel procedures is presented. Complete configurations including external stores can be investigated by a method basically of superposition type. By taking into account various scattering models according to the size and shape of the aircraft's components (surface curvatures, edges, etc.) relative to the impinging radar wavelength, the complete RCS is determined, of which the total radar signature is combined.

The method does not rely on simplified shapes but on an estimation of physical effects typical for curved surfaces, edges, etc. As can be learned from the results for simple bodies, this engineering method can be very helpful for a first guess of the radar signatures of complex configurations during the aerodynamic design procedure. Various other electromagnetic effects can be included also (e.g., cones, corners, phase shifts, etc.) to enhance the capabilities.

However, it should be noted that the procedure is restricted to first-order approximations since more detailed electromagnetic phenomena (e.g., multireflections, interference effects, creeping waves, etc.) are neglected. For those cases, methods based on more complex mathematical approaches should be consulted.

Acknowledgements

I would like to thank Dr. J. Grashof and Dr. H. Niemitz for their profound help in discussions on the subject.

References

- Ball, R.E., *The Fundamentals of Aircraft Combat Survivability Analysis and Design*, AIAA Education Series, New York, 1985.
- Skolnik, M.I., *Radar Handbook*, McGraw-Hill, New York, 1970.
- Ruck, G. T., Barrick, D. E., Stuart, W. D., and Krichbaum, C. K., *Radar-Cross-Section Handbook*, Vols. I and II, Plenum, New York and London, 1970.
- Crispin, J. W. and Siegel, K. M., *Methods of Radar-Cross-Section Analysis*, Academic, New York, 1968.
- Fuhs, A. E., *Radar Cross Section Lectures*, AIAA, New York, 1983.
- Hitzel, S. M., "Aerodynamik und Radar-Signatur," Dornier Note BF30-2813/85, 1985.
- Wooldridge, E. T., *Winged Wonders, The Story of the Flying Wing*, 2nd ed., Smithsonian Institution Press, Washington, DC, 1985, pp. 70-71.
- Oberdörffer, E., "Interne Waffenanbringung bei Luftangriffslugzeugen," DGLR-Jahrestagung, DGLR 85-133, 1985.
- Bowman, J. J., Senior, T. B. A., and Uslenghi, P. L. E., *Electromagnetic and Acoustic Scattering by Simple Shapes*, North-Holland Publishing, Amsterdam, 1969, pp. 400-401.
- Stadmore, H. A., "Radar-Cross-Section Fundamentals for the Aircraft Designer," AIAA Paper 79-1818, Aug. 1979.
- Mitra, R., *Computer Techniques for Electromagnetics*, Pergamon, New York 1973, pp. 160-264.
- Sacher, P., "Analysis of Supersonic Flow for Fighter Application," presented at AGARD-Symposium on Technology for Sustained Supersonic Cruise and Maneuver, Brussels, Oct. 1983.
- Lucchi, C. W., "Ein Panelverfahren höherer Ordnung für kompressible Unterschallströmung," Dornier Note 78/13 B, 1978.